Int. J. Heat Mass Transfer. Vol. 15, pp. 301–314. Pergamon Press 1972. Printed in Great Britain

THE PREDICTION OF LAMINARIZATION WITH A TWO-EQUATION MODEL OF TURBULENCE

W. P. JONES and B. E. LAUNDER

Dept. of Mechanical Engineering, Imperial College, Exhibition Road, London S.W.7, England

(*Received* 18 *December* 1970 *and in revised form* 17 *May* 1971)

Abstract—The paper presents a new model of turbulence in which the local turbulent viscosity is determined from the solution of transport equations for the turbulence kinetic energy and the energy dissipation rate. The major component of this work has been the provision of a suitable form of the model for regions where the turbulence Reynolds number is low.

The model has been applied to the prediction of wall boundary-layer flows in which streamwise accelerations are so severe that the boundary layer reverts partially towards laminar. In all cases, the predicted hydrodynamic and heat-transfer development of the boundary layers is in close agreement with the measured behaviour.

NOMENCLATURE

A^+, a constant appearing in the Van Driest formula for effective viscosity;

c_f, skin friction coefficient $\tau_w/\frac{1}{2}\rho u^2{}_G$;

c_p, specific heat at constant pressure;

c_1, c_2, c_μ } empirical constants appearing in $k-\varepsilon$ turbulence model;

f_1, f_2, f_μ } empirical functions of turbulence Reynolds number appearing in $k-\varepsilon$ turbulence model;

H, shape factor:

$$\int_0^\infty (1-u/u_G)\,\mathrm{d}y \Big/ \int_0^\infty \frac{u}{u_G}\left(1-\frac{u}{u_G}\right)\mathrm{d}y;$$

K, acceleration parameter: $(\nu/u^2{}_G)\,\mathrm{d}u_G/\mathrm{d}x$;

k, turbulence kinetic energy,

$$\frac{\overline{(u'^2+v'^2+w'^2)}}{2};$$

k_T, turbulent thermal conductivity;

l, characteristic turbulence length scale;

l_m, mixing length;

R, Reynolds number of turbulence, $\rho(k^{\frac{1}{2}}l/\mu)$;

R_{ij}, two point velocity correlation at point $\overline{\rho u_i'(p)u_j'(p+\xi_j)}$ where ξ_j has components ξ_1, ξ_2 and ξ_3;

R_2, momentum thickness Reynolds number,

$$\rho\frac{u_G}{\mu}\int_0^\infty \frac{u}{u_G}(1-u/u_G)\,\mathrm{d}y;$$

t, time;

u, local mean velocity parallel to wall;

u_τ, friction velocity $(\tau_w/\rho)^{\frac{1}{2}}$;

u^+, dimensionless value of u: u/u_τ;

u', fluctuating velocity parallel to wall in the mean flow direction;

v', fluctuating velocity normal to the wall;

w', fluctuating velocity parallel to wall and normal to the mean flow direction;

x, Cartesian coordinate in the mean flow direction;

y, Cartesian coordinate normal to the wall;

y^+, dimensionless value of y: $u_\tau y/\nu$;

Greek letters

ε, rate of dissipation of turbulence kinetic energy;

κ, Von Kármán mixing-length constant;

μ, dynamic viscosity;
ν, kinematic viscosity;
ρ, density;
σ, Prandtl number;
τ, total shear stress: $\mu(\partial u/\partial y) - \rho\overline{u'v'}$.

Subscripts
G, free boundary of the layer;
w, wall;
T, turbulent;
i, j, suffices taking values 1, 2 and 3.

1. INTRODUCTION

The phenomenon in question

THE BEHAVIOUR of turbulent boundary layers in accelerating flows is a subject which has attracted a number of experimental examinations in recent years. The most important finding to be established by these studies is that, when the acceleration is severe enough, the originally turbulent layer undergoes a reversion towards laminar [2–6]. The phenomenon has been variously styled "laminarization", "reverse-transition", "inverse-transition" and "re-laminarization"; the first of these is the term adopted in the present paper.

The majority of the measurements of strongly accelerated boundary layers have been of highly non-equilibrium flows; that is, of flows where the structure undergoes rapid evolution in the direction of flow. In these cases it is not possible to ascribe a single parameter to denote precisely when laminarization will occur. However, it is well established that when the acceleration is of sufficient magnitude for the parameter K, defined as $(\nu/u_G^2)\, du_G/dx$, to exceed about 3×10^{-6}, a reversion to laminar flow will eventually ensue. It is noted that accelerations at least an order of magnitude larger than the above commonly arise in rocket nozzles and in flow over turbine blades; the phenomenon thus has substantial practical importance.

Measurements of local Stanton numbers in accelerating flow provide a sensitive indicator of the occurrence of laminarization. The data of Moretti and Kays [3] for example, show a rapid fall of Stanton number in regions of severe acceleration and a corresponding rise downstream therefrom where the boundary layer reverts back to turbulent again. However, their data showed detectable dips in the Stanton number even for accelerations where K did not exceed 10^{-6}; that is, barely one third of the value required to cause a complete degeneration of the turbulent flow towards laminar. More recent measurements of the mean velocity profiles in equilibrium accelerating flows (Launder and Stinchcombe [7], Jones [8], Loyd, Moffat and Kays [9]) have traced the cause of these pre-laminarization dips: over a range of accelerations, while the boundary layer remains essentially turbulent, the viscous sublayer becomes progressively thicker (in terms of y^+) as K is increased, thereby increasing the thermal resistance of this near-wall region.

Prediction of laminarization

The development, in the past few years, of computational procedures for solving the partial differential equations governing two-dimensional boundary layers has enabled attention to be directed to modelling the turbulent transport processes. The first extensive exploration of the capabilities of a turbulence model appears to have been provided by Patankar and Spalding [11]. They showed that the Prandtl mixing-length hypothesis, could be employed to provide accurate predictions of a wide variety of boundary-layer flows. Their predictions of Moretti and Kays' data, however, failed to display any dip in regions of rapid acceleration; as a result the predicted heat-transfer rates at the end of the acceleration were typically twice as high as the measured values.

We have said above that the cause of the diminished level of Stanton number may be attributed to the progressive thickening of the viscous layer in the accelerated region. For this reason we may expect imperfections in the prescription of the turbulence model in the viscosity-dependent sublayer to be the primary cause of

departures between experiment and prediction. Patankar and Spalding employed algebraic wall functions for this region which were based on a modification to the Van Driest proposal [10]. They supposed that the mixing length, l_m, was modified by viscosity according to the formula:

$$l_m = \kappa y\left[1 - \exp - \sqrt{\left(\frac{\tau}{\rho}\right)} y/\nu A^+\right] \quad (1)$$

where, following Van Driest, A^+ was ascribed the constant value, 26. The turbulent viscosity μ_T was then obtained from the mixing length relation:

$$\mu_T = \rho l_m^2 \left|\frac{\partial u}{\partial y}\right|; \quad (2)$$

and the turbulent thermal conductivity, k_T, deduced from the supposition that

$$\sigma_T \equiv \frac{\mu_T c_p}{k_T} = 0{\cdot}9. \quad (3)$$

For both momentum and heat transport, the total effective transport coefficients were taken as the sum of the laminar and turbulent values.

More recently, numerous workers have proposed modifications to the Van Driest hypothesis which purport to provide more universally valid mixing-length distribution. These proposals have included: making A^+ a function of the local dimensionless pressure gradient or mass-transfer rate [12, 13]; replacing τ, in the exponential term of equation (1) by a Couette-flow expression [14]; determining A^+ by way of an ordinary differential equation which describes its rate of change in the stream-wise direction [15, 16]. While a number of the above proposals do represent an improvement on equation (1), there appears to be no evidence that a wholly satisfactory prescription of l_m has yet been devised.

The present contribution

It is proper that the problem of devising more accurate prescriptions of the near-wall variation of mixing-length should continue to attract attention. However, it is well to recall that, in flow over turbine blades, accelerations occur which are several times greater than in the experiments set up in the laboratory, by reference to which turbulence models are assessed. Moreover, besides mass transfer through the blade wall (for transpiration-cooled blades), there will be large variations in temperature, and hence of viscosity and density, normal to the wall; and the effects of stream-line curvature and high free-stream turbulence intensities may be expected to appreciable. It may plausibly be argued that, for such complex flows, a model as simple as the mixing-length hypothesis will never provide the degree of predictive accuracy that a designer needs.

With the above considerations in mind, the authors have embarked on the task of providing a more elaborate description of the turbulent motion than is embodied in the mixing length model. The path taken is similar to that adopted by Ng and Spalding [17], Rodi and Spalding [18], Spalding [19] and Harlow and Nakayama [22] wherein convective transport equations are solved for two scalar properties of turbulence from which characteristic velocity and length scales of the turbulence may be deduced.

The present model is most closely related to Harlow and Nakayama's; for, like these authors, we calculate the turbulence length scale by solving a transport equation for the dissipation rate of turbulence energy. Moreover, each model contains proposals for the way in which molecular viscosity exerts direct influence on the turbulence when the turbulent Reynolds number is low* (it is the inclusion of these Reynolds-number effects which is crucial for the prediction of laminarizing flows). But though the general approach is the same in each model, the detailed proposals are substantially different. The only wall flow for which Harlow and Nakayama provided predictions was flow in a pipe; here agreement with data was poor and the discrepancies suggested that it was their low-

* By comparison, the models of Spalding and his co-workers are limited to regions of flow where the Reynolds number is high.

Reynolds-number proposals which were chiefly at fault.

The present model has undergone a substantially wider program of testing. When applied to the prediction of non-equilibrium flows in strongly negative pressure gradients, the predictions faithfully reproduce the observed reversion towards laminar flow and the consequent diminishing of the Stanton number.

2. THE TURBULENCE MODEL

The high-Reynolds-number form of the model

In the present paper it is assumed that the turbulent shear stress is related to the mean rate of strain via a turbulent viscosity, i.e.

$$-\rho\overline{u'v'} = \mu_T \frac{\partial u}{\partial y}.$$

Following the practice of several workers (e.g. [20]), we take the turbulent viscosity to be determined uniquely by the local values of density, turbulence kinetic energy, k and a turbulence length scale, l. Thus for dimensional homogeneity:

$$\mu_T = c'_\mu \rho k^{\frac{1}{2}} l \tag{4}$$

where c'_μ is a constant. In the present model an equation for k is solved, and the length scale is determined from the solution of an equation for the rate of dissipation of turbulence kinetic energy, ε. Hanjalic [21] has found that the following form of the k and ε equations may provide the basis for satisfactory predictions of a diversity of *high Reynolds-number flows* both near to and remote from walls.

Turbulence energy

$$\rho\frac{Dk}{Dt} = \frac{\partial}{\partial y}\left(\frac{\mu_T}{\sigma_k}\frac{\partial k}{\partial y}\right) + \mu_T\left(\frac{\partial u}{\partial y}\right)^2 - \rho\varepsilon. \tag{5}$$

Energy dissipation

$$\rho\frac{D\varepsilon}{Dt} = \frac{\partial}{\partial y}\left(\frac{\mu_T}{\sigma_\varepsilon}\frac{\partial \varepsilon}{\partial y}\right) + c_1\frac{\varepsilon}{k}\mu_T\left(\frac{\partial \mu}{\partial y}\right)^2 - c_2\frac{\rho\varepsilon^2}{k}. \tag{6}$$

At high Reynolds numbers, ε may be assumed proportional to $\rho k^{\frac{3}{2}}/l$; equation (4) may thus be recast as:

$$\mu_T = c_\mu \rho k^2/\varepsilon \tag{7}$$

where c_μ is a constant.

Equation (5)–(7) represent the limiting form to which the present model reduces in regions where the direct influence of molecular viscosity is negligible. The model contains five empirical constants which are assigned the values given in Table 1.

Table 1. The values of the empirical constants in the high-Reynolds-number form of the k ~ ε *model of turbulence*

c_μ	c_1	c_2	σ_k	σ_ε
0·09	1·55	2·0	1·0	1·3

The terms containing σ_k and σ_ε in equations (5) and (6) represent respectively the diffusion rates of k and ε. These constants therefore possess the significance of turbulent Prandtl numbers for the transport processes in question; that their values should lie close to unity accords with expectations.

The model at low turbulence Reynolds numbers

In order to provide predictions of the flow within the viscous layer adjacent to the wall, the form of the model given above must be enlarged in three ways. These are:

(i) viscous diffusion of k and ε must be included.
(ii) the terms containing the c's in equations (6) and (7) will become dependent upon the Reynolds number of turbulence.
(iii) further terms must be added to account for the fact that the dissipation processes are not isotropic.

The complete form of the turbulence model used in this work is given below and this is

* Hanjalic [21] adopted slightly different values of the constants from those quoted in Table 1 ($c_\mu = 0{\cdot}07$, $c_1 = 1{\cdot}45$ and $\sigma_\varepsilon = 1{\cdot}1$). In practice, the difference between predictions obtained with his constants and with those used here is barely discernible.

followed by a discussion of the terms contained therein.

Turbulence energy

$$\rho\frac{Dk}{Dt} = \frac{\partial}{\partial y}\left[\left(\mu + \frac{\mu_T}{\sigma_k}\right)\frac{\partial k}{\partial y}\right] + \mu_T\left(\frac{\partial u}{\partial y}\right)^2 - \rho\varepsilon - 2\mu\left(\frac{\partial k^{\frac{1}{2}}}{\partial y}\right)^2. \quad (8)$$

Energy dissipation

$$\rho\frac{D\varepsilon}{Dt} = \frac{\partial}{\partial y}\left[\left(\mu + \frac{\mu_T}{\sigma_\varepsilon}\right)\frac{\partial \varepsilon}{\partial y}\right] + c_1 f_1 \cdot \frac{\varepsilon}{k}\mu_T\left(\frac{\partial u}{\partial y}\right)^2 - c_2 f_2 \frac{\rho\varepsilon^2}{k} + 2{\cdot}0\,\mu\mu_T\left(\frac{\partial^2 u}{\partial y^2}\right). \quad (9)$$

Turbulent viscosity formula

$$\mu_T = c_\mu f_\mu \rho k^2/\varepsilon. \quad (10)$$

Turbulent thermal conductivity formula

$$k_T = c_p \mu_T/0{\cdot}9. \quad (11)$$

In the above equation set, the c's and the σ's retain the values assigned to them in Table 1; the influence of Reynolds number mentioned under (ii) above is introduced by way of the f's which are assigned the following forms:

$$\left.\begin{aligned} f_1 &= 1{\cdot}0 \\ f_2 &= 1{\cdot}0 - 0{\cdot}3\exp(-R^2) \\ f_\mu &= \exp[-2{\cdot}5/(1 + R/50)] \end{aligned}\right\} \quad (12)$$

where $R \equiv \rho k^2/\mu\varepsilon$ may be interpreted as the Reynolds number of turbulence. As equation (12) indicates, we have, at present, been able to detect no advantage from making f_1 a function of R.

The viscous diffusion terms in equations (8) and (9) (i.e. $\mu\,\partial k/\partial y$ and $\mu\,\partial\varepsilon/\partial y$) are "exact" in so far as they appear in the exact form of the transport equations for k and ε. The same is not the case, however, with the last term on the right of equation (8). The following argument may serve to indicate the need for some such term and the reason for its precise form.

The need for the term arises from the fact that there are decisive computational advantages from letting ε go to zero at the wall; ε may therefore be interpreted as the isotropic part of the energy dissipation.* Now, the *total* dissipation rate is not zero at the wall; it is given by:

$$\text{Total dissipation}\big|_{y=0} = \nu\left[\left(\frac{\partial \overline{u'}}{\partial y}\right)^2 + \left(\frac{\partial \overline{w'}}{\partial y}\right)^2\right]_{y=0}. \quad (13)$$

Measurements of the instantaneous velocity profile within the viscous sublayer (Bakewell [23]) have shown that at any instant of time the velocity varies linearly with y. This finding implies that u' and w' may be written:

$$\begin{aligned} u' &= a(t)\,y \\ w' &= b(t)\,y \end{aligned} \quad (14)$$

where $a(t)$ and $b(t)$ are functions of time whose mean value is zero. With the insertion of equation (14) into (13) there results:

$$\text{Total dissipation}\big|_{y=0} = \nu\overline{(a^2 + b^2)}. \quad (15)$$

If, further, v', the normal component of fluctuating velocity is presumed negligible, we obtain from equation (5) the following expression for the variation of kinetic energy near the wall:

$$k = \overline{(u'^2 + w'^2)}/2 = \frac{\overline{(a^2 + b^2)}}{2}y^2. \quad (16)$$

From the above result it may readily be deduced

* The total dissipation may be written in terms of a two point velocity correlation tensor as follows:

$$\sum_{i=1}^{3}\sum_{j=1}^{3}\nu\left[\frac{\partial^2 R_{ii}}{\partial\xi_j\,\partial x_j} - \frac{\partial^2 R_{ii}}{\partial\xi_j\,\partial\xi_j}\right]_{\xi_j=0}.$$

The first term is the square brackets is usually negligible for high-Reynolds-number flow regions. the main contribution to ε coming from the second term which is here called the isotropic dissipation and which is exactly zero at the wall.

that

$$2\nu\left(\frac{\partial k^{\frac{1}{2}}}{\partial y}\right)^2 = \nu\overline{(a^2+b^2)}. \tag{17}$$

The equivalence of the right-hand sides of equations (15) and (17) confirms that the new term in equation (9) does indeed reduce to the energy dissipation rate at the wall.

The last term on the right of equation (9) is also one which does not appear in the high-Reynolds-number form of the model. Here the authors can provide no physical argument for its adoption. Its inclusion is simply due to the fact that without it the peak level of turbulence kinetic energy at $y^+ \approx 20$ did not accord with experiment. Several other forms were tried including choosing f_1 to be a function of Reynolds number. The form quoted is however, the only one which generated the desired profile of k near the wall.

To conclude the discussion of the form of the model, it may be helpful to mention the path followed in choosing the Reynolds number functions f_2 and f_μ which appear in equations (9) and (10). The function f_2 was chosen so that the model, when applied to the calculation of the decay of isotropic grid turbulence, accorded with experiment for both high and low turbulence intensities. In order to estimate the form of the function f_μ attention was first confined to the prediction of constant stress Couette flows wherein equation (10) was not used to calculate the turbulent viscosity. Instead μ_T was obtained by way of the Van Driest form of the mixing length formula, equation (1). This practice enabled attention to be focussed simply on the equation for ε which was then adjusted to produce a reasonable turbulent energy distribution in the viscous sublayer region. Thereafter, equation (10) was inverted to provide a preliminary estimate of f_μ:

$$f_\mu = \frac{\mu_T \varepsilon}{\rho k^2 c_\mu}. \tag{18}$$

The algebraic form given in equation (12) provides a variation of f_μ similar to that of the above equation.

Boundary conditions for the turbulence quantities

The following boundary conditions are imposed on the equations for k and ε:

$$\text{at} \quad y = 0; \quad k = 0, \quad \varepsilon = 0. \tag{19}$$

$$\text{at} \quad y = y_G; \quad u_G \frac{\mathrm{d}k_G}{\mathrm{d}x} = -\varepsilon_G \tag{20}$$

$$u_G \frac{\mathrm{d}\varepsilon_G}{\mathrm{d}x} = -c_2 f_2 \varepsilon_G{}^2/k_G \tag{21}$$

where G subscripts denote free-stream conditions.* Equations (20) and (21) are, of course, the limiting free-stream forms of equations (8) and (9) respectively.

Solution of the equations

The governing set of parabolic partial differential equations (comprising equations (8) and (9) together with the mean momentum equation and, for flows involving heat transfer, the stagnation enthalpy equation) have been solved for steady flow conditions by means of a modified version of the finite-difference procedure of Patankar and Spalding [11]. One hundred cross stream intervals were employed of which about half were distributed within the region where y^+ was less than 50. Typically the forward-step size was chosen as 0·3 times the local boundary-layer thickness. Calculations performed with other forward step sizes and various numbers and distributions of cross-stream intervals established that the above values gave sufficient computational accuracy.

For the initial profiles of u, k and ε, required to start the computations, estimated 'fully turbulent profiles' were utilised. In all cases the calculations were started well upstream of the region of interest; as a result, the predictions

* Here, 'free stream' refers to a region sufficiently far from the wall for cross-stream gradients in *all* dependent variables to be negligible.

were found to be little influenced by initial conditions.

3. PRESENTATION AND DISCUSSION OF PREDICTIONS

Figures 1–3 provide comparison between the experimental and predicted properties of the hydrodynamic turbulent boundary layer in zero pressure gradient. In Fig. 1 the predicted mean velocity, turbulence energy and shear stress profiles at a value of $R_2 = 7700$ are compared with Klebanoff's data [24]. Towards the outer edge of the boundary layer, the predicted profiles of k and $\overline{uv}$ do not fall quite as rapidly as the measurements. In other respects, however, the predictions are in excellent accord with the data. Figure 2 displays the variation of boundary-layer shape factor and skin friction coefficient with local Reynolds number, based on the momentum thickness of the boundary layer; comparison is made with Coles' [25] correlations of what he considered to be the most reliable of the available data. For Reynolds numbers greater than $2{\cdot}5 \times 10^3$ the predicted parameters agree with the correlated values within 1 per cent. For Reynolds numbers below this value, however, there is a small but systematic departure of the predictions from the correlations; the predicted shape factor being marginally too high, and the skin friction coefficient rather more noticeably too low. As far as shape factor is concerned, we do not believe the difference is significant considering that, at these low Reynolds numbers, the experimental value of H may be expected to depend on the method of inducing transition.

The principal reason for the discrepancy in skin friction coefficient may be deduced from Fig. 3 which plots the mean velocity profile at several Reynolds numbers in $u^+ \sim y^+$ coordinates. The predicted profiles display a quite detectable Reynolds number dependence within what is usually referred to as the "universal" region of the boundary layer ($50 < y^+ < 200$,

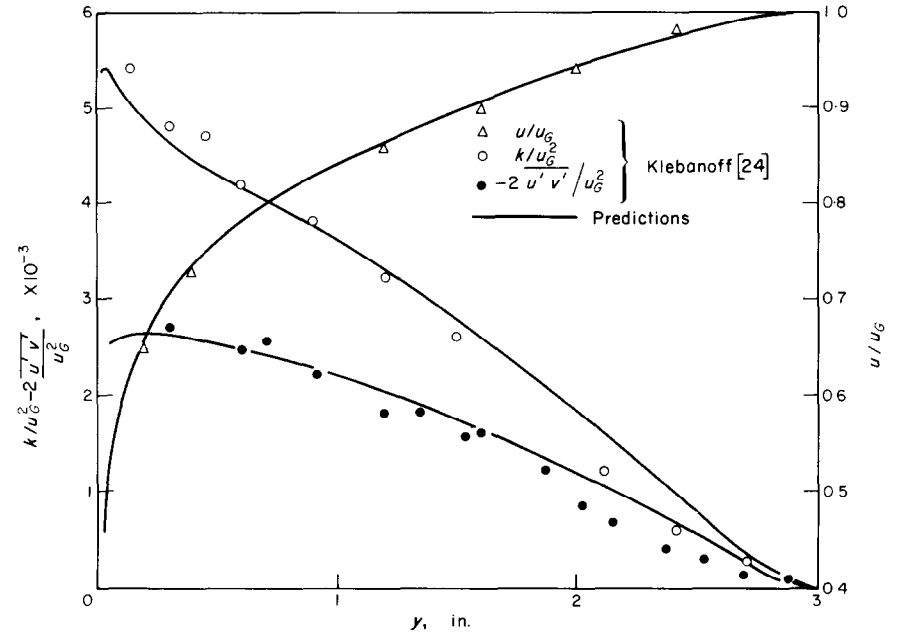

FIG. 1. Boundary layer in zero pressure gradient. Profiles of mean velocity, turbulence energy and shear stress.

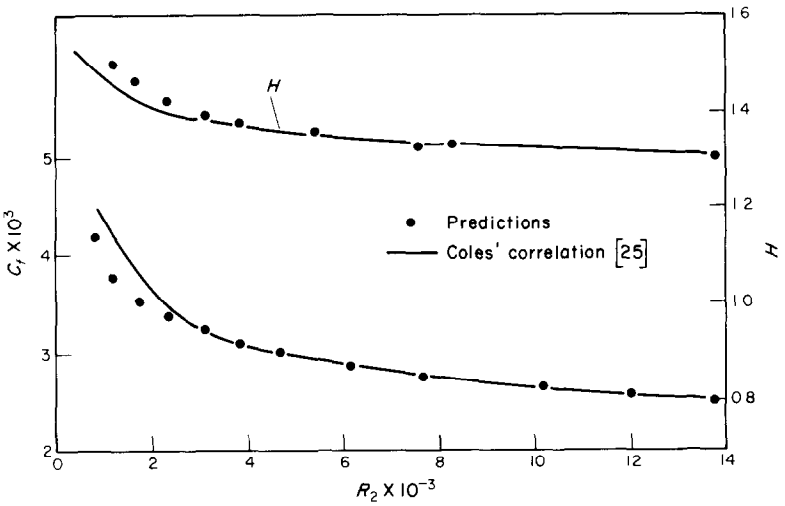

FIG. 2. Boundary layer in zero pressure gradient. Variation of H and c_f vs. R_2.

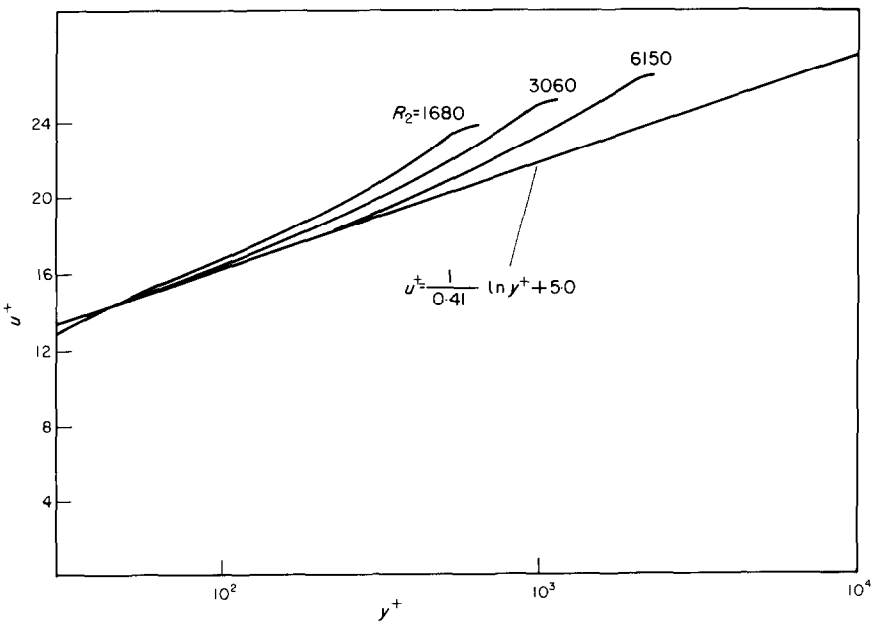

FIG. 3. Boundary layer in zero pressure gradient. Mean velocity profiles in universal coordinates.

say). Now, Coles was guided in estimating the local skin friction coefficients by the notion that the logarithmic region of the boundary layer *was* universal (Fig. 3 includes his proposal for the logarithmic law). If, therefore, the true turbulent boundary layer does possess a Reynolds-number dependence similar to that shown by the predictions, by overlooking this dependence, Coles' estimated values would have been too high by an amount which accords reasonably with the difference between the correlation and the prediction in Fig. 3.

Attention is now directed to accelerating flows; these, it is recalled, provided the motivation for developing the turbulence model presented in Section 2. Firstly, the hydrodynamic predictions of similar sink-flow turbulent boundary layers are considered. Experimentally this type of boundary layer may be realised by accelerating fluid through converging planes. The special relevance of these boundary layers has been discussed in detail elsewhere [7, 12]; here it may suffice to remark that when the self-preserving state is reached, the acceleration parameter, K and the boundary-layer parameters c_f, R_2 and H are all invariant with x.

Figure 4 compares the predicted mean velocity profile for $K = 2{\cdot}2 \times 10^{-6}$ with the measurements of Jones [8]. There is some discrepancy between the detailed shape of the profiles, but the main point of note is that the predictions, like the measurements, show that the velocity profile for $y^+ > 30$ lies considerably *above* the "universal" logarithmic law. By comparison, predictions obtained with the mixing length hypothesis, (with the mixing length near

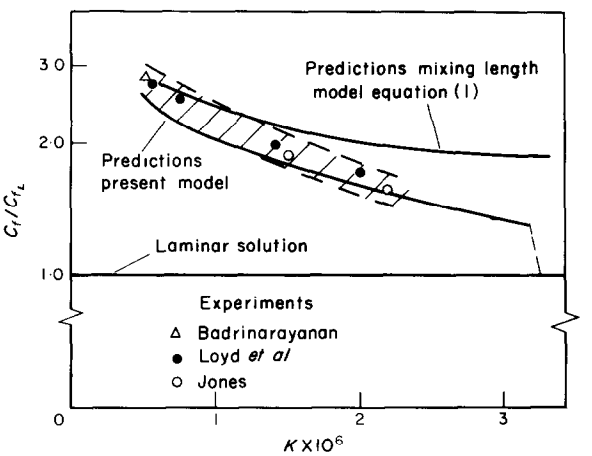

FIG. 5. Sink flow boundary layers. Variation of c_f with K.

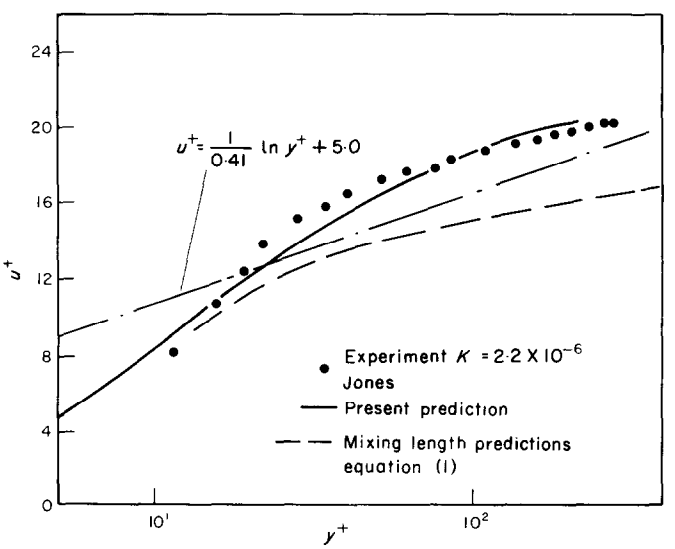

FIG. 4. Sink-flow boundary layers. Mean velocity profiles for $K = 2{\cdot}2 \times 10^{-6}$.

the wall given by equation (1)) fall *below* the logarithmic line.

Figure 5 shows the variation of skin friction with K for sink flow boundary layers. The ordinate c_f/c_{f_L} denotes the value of the local skin friction coefficient divided by the value of c_f for a laminar boundary layer at the same value of K. Here it should be mentioned that the task of determining the value of c_f by experiment is not an easy one. Thus, even though the experimental data lie on a smooth line their accuracy is not certain within a tolerance of about ± 10 per cent (the value quoted by Loyd, Moffat and Kays [9]). The shaded region in Fig. 5 denotes the ± 10 per cent band about a mean line through the data.

From the figure it may be deduced that:

(i) for values of K greater than $1{\cdot}2 \times 10^{-6}$, the present model predicts values of c_f which are within the band of experimental uncertainty (for less severe accelerations the model gives skin friction coefficients which are a few per cent too low).

(ii) for values of K greater than 10^{-6} the mixing-length predictions give values of c_f which are too high, the error increasing rapidly with K.

A particular striking outcome of the predictions with the $k \sim \varepsilon$ model is that for values of K in excess of $3{\cdot}2 \times 10^{-6}$ no turbulent solution exists. That is to say, if one starts the predictions with an initially turbulent boundary layer and then applies the acceleration, the turbulence gradually decays away and the mean velocity profile collapses to that appropriate to laminar flow. To the authors knowledge there is at present no definitive experimental data available that pinpoint the value of K at which degeneration to laminar flow occurs. Some very recent unpublished data of the authors' suggest that for $K = 3{\cdot}0 \times 10^{-6}$ the boundary layer is probably decaying to laminar; but the rate of decay is too slow and the length of the test section too short for any definite conclusions to be drawn at present.

In summarizing the above predictions of equilibrium sink flows, it may be stated that, while detailed discrepancies exist, the overall features, such as the variation of c_f with K, the thickening of the viscous layer and the collapse to a laminar flow for a value of K near 3×10^{-6}, are in accord with experimental data. The measure of agreement achieved may be regarded as a major achievement of the model.

The final (and, from a practical viewpoint, the most important) class of problems to be considered in this paper is that of heat transfer through *non-equilibrium* accelerated boundary layers. Predicted variations of Stanton number are compared with measurements of Moretti and Kays [3] and Filetti [26] in Fig. 6–9. In all the experiments considered, the acceleration is preceded by a development length of between 4 ft and 5 ft in which the free stream velocity is uniform; a step change in wall temperature is applied at $x = 2$ ft and downstream therefrom, the wall temperature is maintained nearly constant.

For Filetti's run (3) and Moretti and Kays' run (42), shown in Figs. 6 and 7, the accelerations were such that the value of K was fairly uniform. with values of about $2{\cdot}0 \times 10^{-6}$ and $3{\cdot}2 \times 10^{-6}$ respectively. In each case there is a marked drop in Stanton number in the region of acceleration and a rise downstream therefrom. The predictions consistently mirror this experimental behaviour though for each test the Stanton numbers are somewhat lower than the measured, even upstream of the acceleration. Indeed, for the data shown in Fig. 6, the largest discrepancy between measurement and prediction (about 15 per cent) occurs in the region $3 \text{ ft} < x < 4 \text{ ft}$ where the pressure gradient is *zero*. To the authors' knowledge all other theoretical models that have been applied to the prediction of this flow exhibit lower values of St than the measured over this region of the flow. In view of this, the present predictions may be deemed to be satisfactory.

For the data shown in Figs. 8 and 9, K varied roughly sinusoidally reaching peak values of

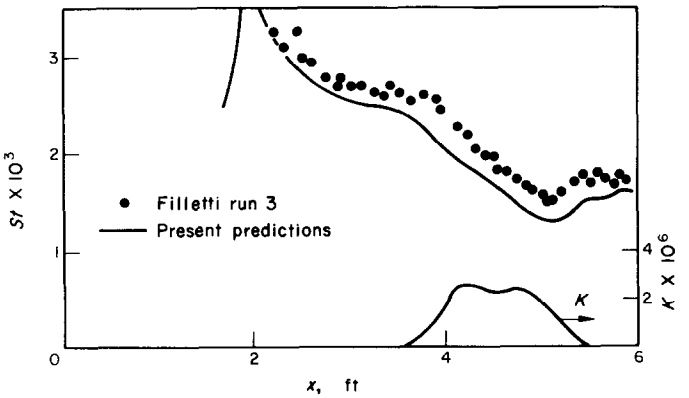

FIG. 6. Variation of St vs. x. Filetti run 3.

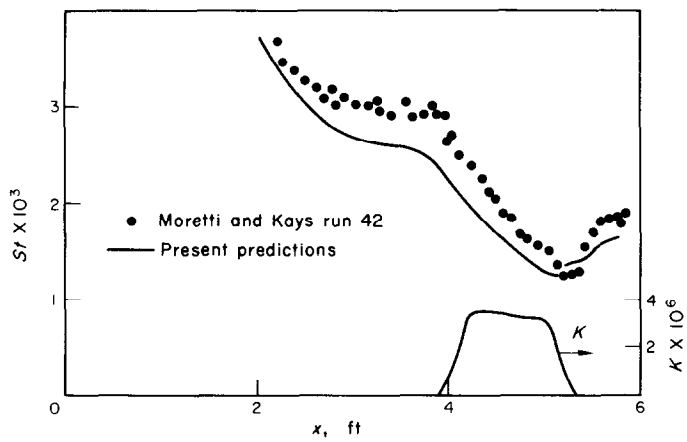

FIG. 7. Variation of St vs. x. Moretti and Kays run 42.

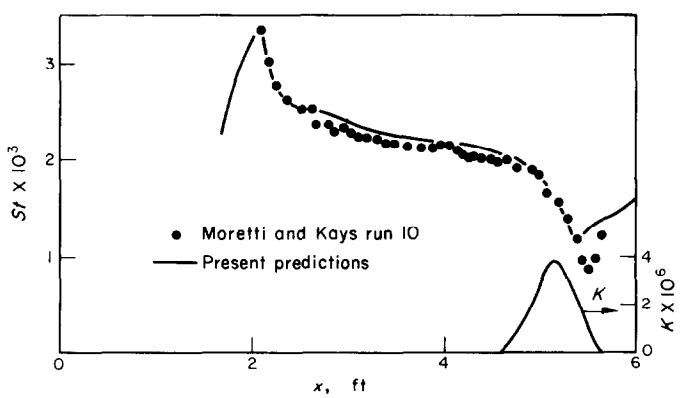

FIG. 8. Variation of St vs. x. Moretti and Kays run 10.

4×10^{-6} and 7×10^{-6} respectively. In Fig. 8 the predictions like the measurements, show a rapid falling off in Stanton number in the region of severe acceleration. The predictions, however, exhibit too rapid recovery as the acceleration dies away. A similar behaviour is displayed in Fig. 9 for the more severe of the accelerations.

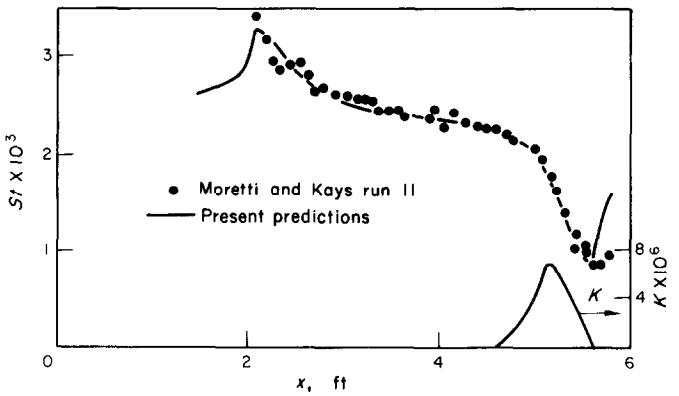

FIG. 9. Variation of St vs. x. Moretti and Kays run 11.

Agreement between measurement and prediction is even better here than in Fig. 8. At the end of the acceleration, however, the predicted boundary layer reverts towards turbulent more quickly than the measurements suggest.

That such a discrepancy should arise is not surprising for, in the last two cases, the accelerations are so severe that the employment of a turbulent-viscosity concept may be expected to lead to shear stresses which are seriously in error.

Notwithstanding its limitations, however, it appears that the present turbulence model provides greater predictive accuracy than any other currently available for strongly accelerated boundary-layer flows. Moreover, because it determines the length scale of turbulence by way of a differential transport equation, it may be expected that the model will be equally successful at taking account of the influence of surface mass transfer and fluid property variations on the hydrodynamic and thermal development of the boundary layer.

4. CONCLUSIONS

1. The paper has presented a turbulence model in which the local value of turbulent viscosity is determined from the solution of transport equations for the turbulence energy and the turbulence-energy-dissipation rate. The main contribution of this research has been the provision of a suitable form for these equations within the region near the wall where viscosity exerts a direct influence on the turbulence structure.

2. The model has been applied to the prediction of a number of strongly accelerated boundary-layer flows. A few detailed discrepancies between experiment and prediction have emerged; but, overall, the model has been shown to be remarkably successful in predicting the hydrodynamic and thermal consequences of the acceleration. The model appears to offer substantially greater predictive accuracy than has so far been achieved with mixing-length models.

3. More extensive testing of the model is needed particularly for flows in which surface

mass fluxes and fluid property variation are substantial.

ACKNOWLEDGEMENTS

The research reported herein has been supported by the Science Research Council under Contract No. B/SR/5049.

All the numerical computations have been performed by means of digital computers under the control of the University of London Computing Centre.

REFERENCES

1. B. E. LAUNDER, Laminarisation of the turbulent boundary layer by acceleration, M.I.T. Gas Turbines Lab. Rep. No. 77 (1964).
2. B. E. LAUNDER, Laminarization of the turbulent boundary layer in severe acceleration, *J. Appl. Mech.* **31**, 707 (1964).
3. P. M. MORETTI and W. M. KAYS, Heat transfer through an incompressible turbulent boundary layer with varying free stream velocity and varying surface temperature, Stanford University, Thermo Sci. Div. Rep. PG-1 (1965).
4. F. A. SCHRAUB and S. J. KLINE, A study of the structure of the turbulent boundary layer with and without longitudinal pressure gradients, Stanford University, Thermo. Sci. Div. Rep. MD-12 (1965).
5. M. A. BADRI NARAYANAN and V. RAMJEE, On the criteria of reverse transition in a two dimensional boundary layer flow, India Inst. of Sci. Rep. AE 68 FMI (1968).
6. V. C. PATEL and M. R. HEAD, Reversion of turbulent to laminar flow, Aero. Res. Counc. 29 859–F.M. 3929 (1968).
7. B. E. LAUNDER and H. S. STINCHCOMBE, Non-normal similar boundary layers, Imperial College, Mech. Eng. Dept. Rep. TWF/TN/21 (1967).
8. W. P. JONES, Strongly accelerated turbulent boundary layers, M.Sc. Thesis, Imperial College (1967).
9. R. J. LOYD, R. J. MOFFAT and W. M. KAYS, The turbulent boundary layer on a porous plate: an experimental study of the fluid dynamics with strong favourable pressure gradients and blowing, Stanford University, Thermo. Sci. Div. Rep. No. HMT-13 (1970).
10. E. R. VAN DRIEST, On turbulent flow near a wall, *J. Aero. Sci.* **23**, 1007 (1957).
11. S. V. PATANKAR and D. B. SPALDING, *Heat and Mass Transfer in Boundary Layers*. Morgan-Grampian Press, London (1967).
12. B. E. LAUNDER and W. P. JONES, Sink flow turbulent boundary layers, *J. Fluid Mech.* **38**, 817–831 (1969).
13. T. E. POWELL and A. B. STRONG, Calculation of the two-dimensional turbulent boundary layer with mass addition and heat transfer, Proceedings of the 1970 Heat Transfer and Fluid Mechanics Institute (1970).
14. T. CEBECI, A. M. O. SMITH and G. MOSINSKIS, Solution of the incompressible turbulent boundary layer equations with heat transfer, *J. Heat Transfer* **92C**, 113–143 (1970).
15. W. P. JONES and B. E. LAUNDER, On the prediction of laminarescent turbulent boundary layers, ASME paper 69-HT-13 (1969).
16. W. M. KAYS, R. J. MOFFAT and W. H. THIELBAHR, Heat transfer to the highly accelerated turbulent boundary layer with and without mass addition, *J. Heat Transfer* **92C**, 499 (1970).
17. K. H. NG and D. B. SPALDING, Some applications of a model of turbulence for boundary layers near walls, Imperial College, Mech. Eng. Rep. BL/TN/A/14 (1969).
18. W. RODI and D. B. SPALDING, A two parameter model of turbulence and its application to free jets, *Wärme und Stoffübertragung Bd.* **3** S.85–95 (1970).
19. D. B. SPALDING, Concentration fluctuations in a round jet, *Chem. Engng Sci.* **26**, 95 (1971).
20. H. W. EMMONS, Shear flow turbulence, Proc. 2nd U.S. National Congress App. Mech. ASME (1954).
21. K. HANJALIC, Two dimensional asymetrical turbulent flow in ducts, Ph.D. Thesis, University of London (1970).
22. F. H. HARLOW and P. I. NAKAYAMA, Transport of turbulence energy decay rate, Los Alamos Sci. Lab. Rep. LA 3854 (1968).
23. H. P. BAKEWELL, Viscous sublayer and adjacent wall region in turbulent flow, *Physics Fluids* **10**, 1880 (1969).
24. P. S. KLEBANOFF, Characteristics of turbulence in a boundary layer with zero pressure gradient, N.A.C.A., TN 3178 (1954).
25. D. E. COLES, The turbulent boundary layer in a compressible fluid, Rand Rep. R 403, PR (1962).
26. E. G. FILETTI, University of Standford unpublished report, data quoted by MORETTI and KAYS (3) (1965).

PRÉDICTION DE LAMINARISATION AVEC UN MODÈLE DE TURBULENCE À DEUX ÉQUATIONS

Résumé—L'article présente un nouveau modèle de turbulence dans lequel la viscosité turbulente locale est déterminée à partir de la solution des équations de transport pour l'énergie cinétique de turbulence et la vitesse de dissipation d'énergie. La majeure partie de ce travail a été l'élaboration d'une forme adéquate du modèle pour des régions où le nombre de Reynolds de turbulence est faible.

Le modèle a été appliqué à la prédiction des écoulements à couche limite à la paroi dans lesquels des accélérations longitudinales sont si fortes que la couche limite redevient partiellement laminaire. Dans tous les cas, le développement hydrodynamique et thermique prévu des couches limites est en parfait accord avec le comportement observé.

DIE BESTIMMUNG DER LAMINARISIERUNG MIT EINEM AUS ZWEI GLEICHUNGEN BESTEHENDEN TURBULENZMODELL

Zusammenfassung—Die Arbeit behandelt ein neuse Turbulenzmodell, bei dem die örtliche turbulente Zähigkeit aus der Lösung der Transportgleichungen für die kinetische Energie der Turbulenz und der Energiedissipation bestimmt wird. Der Hauptteil dieser Arbeit bestand darin, eine passende Form des Modells für Bereiche zu schaffen, in denen die Reynoldszahl der Turbulenz niedrig ist.

Das Modell ist auf die Bestimmung von Wandgrenzschichtströmungen angewandt worden, bein denen so starke Beschleunigungen in Strömungsrichtung auftreten, dass die Grenzschicht teilweise in den laminaren Bereicht umschlägt. In allen Fällen ist die berechnete Entwicklung der hydrodynamischen und thermischen Grenzschicht in guter Übereinstimmung mit dem gemessenen Verhalten.

РАСЧЕТ ЛАМИНАРИЗАЦИИ С ПОМОЩЬЮ МОДЕЛИ ТУРБУЛЕНТНОСТИ, СОСТОЯЩЕЙ ИЗ ДВУХ УРАВНЕНИИ

Аннотация—В статье представлены новая модель турбулентности, в которой локальная турбулентная вязкость определяется из решения уравнений переноса для кинетической энергии турбулентности и скорости диссипации энергии. Основной задачей данной работы было создание соответствующего вида модели для областей с малым турбулентным числом Рейнольдса.

Модель использовалась для расчета течений в пограничном слое на стенке где ускорения настолько сильны, что пограничный слой частично обращается в ламинарный. Во всех случаях расчетные гидродинамические и теплообменные разработки для пограничных слоев хорошо согласуются с измеренными значениями.